Alzheimer's & Dementia: Diagnosis, Assessment & Disease Monitoring 11 (2019) 257-263

Special Section: Blood-Based Biomarkers for Alzheimer's Disease & Related Dementias

Aβ and tau structure-based biomarkers for a blood- and CSF-based two-step recruitment strategy to identify patients with dementia due to Alzheimer's disease

Andreas Nabers[a], Henning Hafermann[b], Jens Wiltfang[c,d,e,**], Klaus Gerwert[a,*]

[a]Department of Biophysics, Ruhr-University Bochum, Bochum, Germany
[b]LVR-Hospital Essen, Department of Psychiatry and Psychotherapy, Faculty of Medicine, University of Duisburg-Essen, Essen, Germany
[c]Department of Psychiatry and Psychotherapy, University Medical Center Goettingen (UMG), Georg-August-University Goettingen, Göttingen, Germany
[d]German Center for Neurodegenrative Diseases (DZNE), Göttingen, Germany
[e]iBiMED, Medical Sciences Department, University of Aveiro, Aveiro, Portugal

Abstract

Introduction: Alzheimer's disease (AD) diagnosis requires invasive CSF analysis or expensive brain imaging. Therefore, a minimal-invasive reliable and cost-effective blood test is requested to power large clinical AD trials at reduced screening failure.

Methods: We applied an immuno-infrared sensor to measure the amyloid-β (Aβ) and tau secondary structure distribution in plasma and CSF as structure-based biomarkers for AD (61 disease controls, 39 AD cases).

Results: Within a first diagnostic screening step, the structure-based Aβ blood biomarker supports AD identification with a sensitivity of 90%. In a second diagnostic validation step, the combined use of the structure-based CSF biomarkers Aβ and tau excluded false-positive cases which offers an overall specificity of 97%.

Discussion: The primary Aβ-based blood biomarker funnels individuals with suspected AD for subsequent validation of the diagnosis by structure-based combined analysis of the CSF biomarkers Aβ and tau. Our novel two-step recruitment strategy substantiates the diagnosis of AD with a likelihood of 29.

Keywords: Alzheimer's disease; Amyloid-beta; Tau; Protein misfolding; Diagnostics

1. Introduction

Alzheimer's disease (AD) pathology is accompanied by misfolding of amyloid-β (Aβ) and tau from monomeric into β-sheet–enriched pathogenic species. This process is suggested to precede about 10-15 years before clinical onset of the disease [1,2]. The aggregated Aβ and tau isoforms result in macroscopic plaques and neurofibrillary tangles in the brain of patients with AD [3,4]. So far, guidelines and actual recommendations for AD diagnosis intend the quantitative analysis of CSF biomarkers and additional imaging methods such as amyloid positron emission tomography (Amyloid-PET) to detect and correlate Aβ burden in the brain with AD pathology [5–10]. These techniques require either invasive lumbar punctures or expensive PET analyses, which rely on the use of radioactive compounds. Thus, there is a general agreement that a minimal-invasive, reliable, and cost-effective blood test is requested as a first screening funnel to identify individuals with high risk for AD [11–15]. To date, only few blood tests present the potential to detect AD [16–19].

Conflict of interest: The authors declare no competing financial interest.

*Corresponding author. Tel.: +49(0)2343224462; Fax: +49(0)2343214238.

**Corresponding author. Tel.: +49(0)5513966601; Fax: +49(0)5513922798.

E-mail address: jens.wiltfang@med.uni-goettingen.de (J.W.), klaus.gerwert@bph.rub.de (K.G.)

https://doi.org/10.1016/j.dadm.2019.01.008

Already in 2016, we have shown that the secondary structure distribution of Aβ in blood plasma, measured by an immuno-infrared sensor, is an excellent biomarker for AD, reflecting the Aβ burden in the brain [20,21]. In contrast to quantitative ELISA assays, the immuno-infrared sensor does not detect the concentration decline of Aβ42, which is a secondary event associated with Aβ42 deposition in the brain, but directly monitors the misfolding of Aβ, which is proposed to be a primary event in AD pathology occurring 15-20 years before clinical onset. We propose that our structure-based biomarker offers a unique additional molecular feature to the use of Aβ peptide ratios as promising AD biomarkers. Because β-sheet–enriched misfolding of Aβ peptides is thought to be an initial event in the pathophysiological cascade of AD, our immuno-infrared sensor is promising to identify patients at risk for AD at an early preclinical stage [22]. Recently, we have validated the diagnostic performance of our structure-based biomarker for mild to severe AD, prodromal AD, and for preclinical AD in three independent clinical studies [20,22]. We also demonstrated in the latter studies that the Aβ secondary structure distribution as structure-based AD biomarker correlates significantly with already well established standard CSF core biomarkers (Aβ42/40 ratio, total-tau (ttau), phospho-tau181 [ptau]) and neuroimaging (Amyloid-PET) biomarkers of AD. Most remarkable, in a 15-year longitudinal aging study comprising 10,000 participants, we identified in a subcohort of 890 healthy participants, 48 of 65 participants who subsequently developed AD. We predicted AD progression in participants without any cognitive symptoms in an average of 8 years before their clinical onset with a sensitivity of 71% and specificity of 91% [22].

To increase the sensitivity of the structure-based blood biomarker for screening applications, we shift the diagnostic threshold within our novel two-step recruitment strategy to higher wavenumbers which yielded more false-positive cases at reduced specificity. Within a second validation test, the specificity could be increased by immuno-infrared sensor–based CSF analysis to exclude false-positive cases. A majority vote classifier was applied to categorize all CSF samples and to exclude false-positive cases. Here, we present the performance of the novel two-step AD recruitment strategy which preselects subjects at risk for AD by the blood-based immuno-infrared sensor screening assay. Individuals to be at risk for AD according to the blood-based immuno-infrared sensor screen underwent subsequently CSF-based analyses of the Aβ peptide and tau conformation. Here, in addition to Aβ, tau also was used as a structure-based biomarker. This two-step AD recruitment strategy provides an overall sensitivity of 87% and specificity of 97%. In principle, the structure-based blood screen is promising to identify preclinical and prodromal AD, which subsequently can be studied by CSF biomarkers and/or Amyloid-PET to validate the screen diagnosis. However, the blood screen test preselected 59 of 100 subjects, whereas 34 of 39 cases were correctly classified as AD according to the clinical diagnosis. Only two cases were misdiagnosed as false-positive cases.

2. Methods

2.1. Participants and clinical phenotyping

The prospective study fulfills the international standards for studies of diagnostic test accuracy in dementia [23].

For the present study, 61 disease control (DC) subjects and 39 AD cases were acquired from a prospective study designed and initiated by the gerontopsychiatric unit of the department of psychiatry and psychotherapy at the LVR Clinics, University of Duisburg-Essen, between 2009 and 2013 (PI J.W.). The study was approved by the ethical board of the University of Duisburg-Essen (ID 12 5160 BO) and the research use of the samples and data was in accord with the terms of the informed consents. Sample acquisition and dementia diagnostics were made according to the criteria of the National Institute for Neurological and Communicative Disorders and Stroke and the Alzheimer's Disease and Related Disorders Association and included the 2011 recommendations from the National Institute on Aging. The clinical diagnosis of DC was performed according to the International Classification of Diseases (ICD-10). Patients were investigated by psychometric testing (Mini-Mental State Examination and/or extended neuropsychological evaluation) and CSF-guided neurochemical dementia diagnostics. A detailed description of the clinical cohort can be found in the study by Nabers et al. [20].

Importantly, for all subjects, CSF levels of Aβ40, Aβ42, ttau, ptau, the Aβ42/40 ratio, and demographic data were available (Supplementary Table 1). Gerontopsychiatrists and neuropsychologists had access to all available clinical, neuroimaging, psychometric, and conventional CSF dementia biomarker data but were blinded for the immuno-infrared analysis. The DC group comprised patients with dementia of other origin and nondemented patients with heterogonous neurological or psychiatric diseases but without memory complaints. Most patients with AD presented with early AD.

All CSF samples were assessed with the Meso Scale Discovery (MSD) V-Plex Aβ peptide panel multiplex kit using monoclonal antibody 6E10 for detection (MSD, Rockville, MD). The Aβ peptides Aβ38, 40, and 42 were determined according to the manufacturer's instructions after 16-fold dilution of the CSF samples with "Diluent 35" (MSD). CSF concentrations of ttau and ptau were measured in duplicate by commercially available ELISA in an accredited expert laboratory for CSF-guided neurochemical dementia diagnostics (P. Lewczuk, University of Erlangen-Nürnberg, Germany) [20,24].

2.2. Immuno-infrared sensor workflow

Preparation of the immuno-infrared sensor was described in detail previously [20,22]. Briefly, the sensor surface was

functionalized with monoclonal antibody A8978 (Sigma-Aldrich, Germany) for Aβ detection in blood plasma and CSF and monoclonal antibody TAU-5 for tau detection in CSF, respectively. After surface functionalization, the sensor was saturated to prevent unspecific binding. Finally, Aβ and tau was separately extracted from plasma (200 μL) and/or CSF (50 μL) for 1 hour followed by excessive PBS rinsing for 30 minutes. The recorded amide I absorbance band represented the biomarker secondary structure distribution in the respective body fluid by its maximum frequency. The immuno-infrared sensor technology is detailed in the study by Nabers et al. [20–22].

2.3. Bioinformatics

Before data interpretation, infrared-difference spectra were corrected for water vapor contributions by scaled subtraction as described in detail previously [20,22]. Afterward, the amide I maximum frequency was determined by in-house procedures programmed with MATLAB 2015A (Mathworks). Statistical tests were performed using Origin 2016 (Origin Laboratories). Data distribution and group differences were analyzed with nonparametric Kruskal–Wallis analysis of variance. Thereby, statistical tests were conducted two-sided at a significance level of 0.05. Significance levels are denoted as follows: $*P < .05$, $**P < .01$, $***P < .001$.

For the first diagnostic step based on blood plasma, the decisive threshold for AD and DC differentiation was set to $<1647\ cm^{-1}$ indicative for AD to reveal a sensitivity of ≈90%. For the second diagnostic step, the decisive threshold for all biomarkers was set to $<1643\ cm^{-1}$ determined by receiver operator characteristics (ROC)-curve analysis to reveal the highest diagnostic accuracy for each marker. These ROC-curve analyses were also described in the study by Nabers et al. [20]. Using a simple majority vote classifier, AD diagnosis was confirmed in step-2, as well as most false-positive cases were excluded. Therefore, each of the three biomarkers, Aβ from plasma, Aβ from CSF, and tau from CSF, equally contributed to the decision process of the majority vote classifier. In case the amide I maximum frequency of two biomarkers was below the decisive threshold at $1643\ cm^{-1}$, the final diagnosis was AD. On the other hand, if two biomarkers had a maximum above or equal to $1643\ cm^{-1}$, the classifier decision was non-AD.

3. Results

The Aβ secondary structure distribution in blood plasma was determined by the immuno-infrared assay as described previously [20–22]. Briefly, the sensor element is functionalized with highly specific antibodies recognizing all structural isoforms of Aβ or tau (Supplementary Fig. 1A), including helical or disordered monomers and β-sheet–enriched oligomers, prefibrillar, and fibrillar species. The recorded so-called amide I band represents the C=O stretching vibration of the protein backbone. The wavenumber or frequency of the corresponding absorbance band as shown in Supplementary Fig. 1B reflects the secondary structure distribution of Aβ or tau, respectively. Monomeric alpha-helical or disordered isoforms absorb between 1653 and 1649 wavenumbers (cm^{-1}), whereas β-sheet isoforms absorb around $1626\ cm^{-1}$. Increased β-sheet content, which is characteristic for Aβ and tau in AD pathology, shift the amide I band to lower wavenumbers. The more β-sheet isoforms are present in the blood, the larger is the spectral downshift to lower wavenumbers (Supplementary Fig. 1B). In step 1 of our two-step AD recruitment strategy, total-Aβ was extracted from blood plasma. The amide I frequency indicates the content of β-sheet–enriched, pathogenic Aβ in the total-Aβ fraction.

In the first step, we analyzed blood plasma of 61 DCs and 39 AD cases from a prospective study (Essen, Germany). The study design with SOPs for sample acquisition preanalytical sampling handling, sample storage, as well as diagnostic criteria for clinical phenotyping (including inclusion or exclusion criteria) is summarized in detail elsewhere [20]. AD and DCs differed significantly in the plasma Aβ amide I band frequency at maximum position (Fig. 1, $P < .0001$, two-sided nonparametric Kruskal–Wallis analysis of variance test). Importantly, our structure-based plasma biomarker significantly correlates (Spearman rank correlation with a significance value p for a niveau of $\alpha = 0.05$) with well-established neurochemical CSF biomarkers such as Aβ42/40 ratio ($r_S = 0.47$, P value $= 6 \times 10^{-7}$, determined by MSD), ttau ($r_S = -0.41$, P value $= 3 \times 10^{-5}$, determined by ELISA), and ptau ($r_S = -0.48$, P value $= 7 \times 10^{-7}$, determined by ELISA). We have detailed the analysis of the latter CSF biomarkers elsewhere [20]. However, in our former studies, we established $1643\ cm^{-1}$ as decisive threshold (by ROC curve and Youden's cutoff) to reveal highest test accuracy. But the first diagnostic step, which serves as funnel for subsequent more invasive CSF analyses, should reveal high test sensitivity. To obtain 90% sensitivity, the decisive threshold had to be up-shifted from $1643\ cm^{-1}$ used in former studies [20] to $1647\ cm^{-1}$. The latter threshold up-shift increased the diagnostic sensitivity on the cost of specificity, which dropped to 61% (Fig. 2; step 1) as compared with the clinical diagnosis. In total numbers, we identified 35 of 39 AD cases with the first diagnostic step based on blood plasma; the number of false-positives (FP) was 24 of 61 DC subjects. Four AD cases could not be identified in the first step and thus remained false-negatives. Interestingly, three of the four AD cases that were misclassified in our blood test—as compared with the clinical diagnosis—were also indicated as non AD by Aβ or tau in CSF (see Supplementary Table 1B). In addition, two of this three clinical cases even had normal CSF Aβ42 levels (≥600 pg/mL) as determined by MSD and one of them was cognitively unimpaired (MMSE ≥ 27). Thus, these three cases might be actually misdiagnosed as AD. Prospective follow-up examination

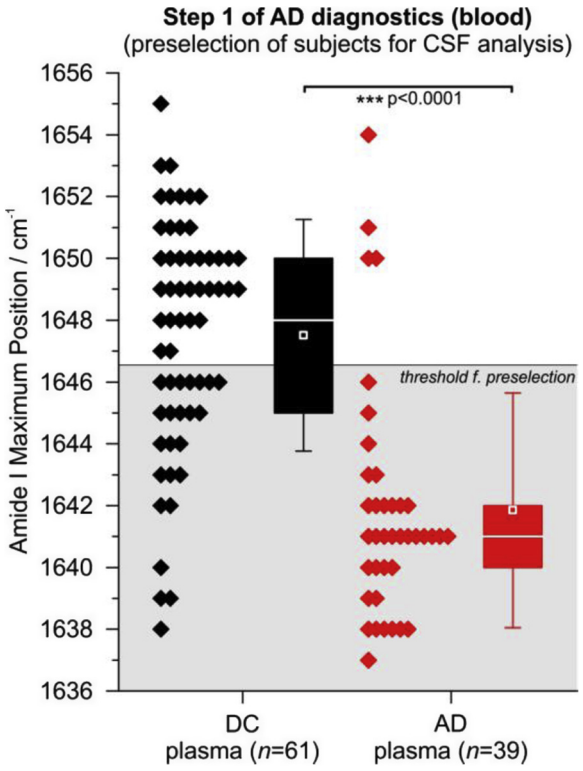

Fig. 1. The Aβ amide I band frequencies of 61 disease controls and 39 AD cases (prospective study, Essen) are shown as diamonds. Aβ was extracted by mAb A8978 from blood plasma. The frequency of the amide I band is the measure of the structure-based biomarker, indicating the Aβ secondary structure distribution in blood plasma. The threshold was shifted to 1647 cm^{-1} (solid horizontal line) to increase the sensitivity to 90%. In former studies, 1643 cm^{-1} was used as decisive threshold for highest test accuracy. By up-shifting the threshold to 1647 cm^{-1}, the specificity dropped from 88% to 61%. The 24 false-positives (FP) and 35 true-positives (TP) (gray background) were further examined in step 2 (Fig. 2, Supplementary Fig. 3) to exclude FP and validate TP. In box plots, 25/50/75% quantiles are shown as horizontal lines, the average amide I band position as square, and ±standard deviation as whiskers. Significant group differences are indicated by *P* value (two-sided nonparametric Kruskal–Wallis analysis of variance test) and by asterisks: ***$P < .001$.

of these subjects is intended in the future to further validate the clinical diagnoses.

In the second diagnostic step, we analyzed CSF samples of the preselected 35 AD cases and 24 FP. Analog to the Aβ analysis from blood plasma, the immuno-infrared assay was now used to separately extract and analyze the Aβ peptide and tau protein secondary structure distribution in CSF (Supplementary Fig. 1). The amide I band frequency of Aβ and tau in CSF of each person are presented in Supplementary Fig. 2 and Supplementary Fig. 4. Especially the tau secondary structure distribution is not suitable as a stand-alone biomarker for AD classification. But the combination of the plasma Aβ data obtained in step one and CSF Aβ and tau values provides a panel of three data sets that were used for validation of the AD diagnosis. For all three biomarker data sets—plasma Aβ, CSF Aβ, and CSF tau—the decisive threshold was set to <1643 cm^{-1} for AD identification as used in our former study [20]. In the second diagnostic step, 1643 cm^{-1} was used as decisive threshold, which was experimentally determined as decisive threshold for highest test accuracy in our former studies, for each biomarker Aβ in plasma, Aβ in CSF, and tau in CSF. Thus, each biomarker was set to provide the maximum accuracy within the majority vote classifier, respectively. Using a simple majority vote classifier, we confirmed the AD diagnosis suggested in step 1 in 34 of 35 (97%) preselected AD cases. Interestingly, the blood test amide I value of the one misclassified participant was directly at the threshold of 1643 cm^{-1} of the assay as used in the study by Nabers et al. [20]. By contrast, the Aβ amide I value in CSF was actually below the threshold indicating AD while tau was above the threshold in CSF (see Supplementary Fig. 4). The clinical diagnosis was early dementia due to AD. This finding might indicate that participants who are just at the border to switch to clinical Alzheimer's showed opposing biomarker states. This observation will be followed up in a more detailed study. However, the second diagnostic step excluded false-positive cases in 22 of 24 subjects (92%) (Fig. 2; step 2). In sum based on both diagnostic steps, 34 AD cases (of 39) and 59 controls (of 61) were classified correctly. Thus, the two-step AD recruitment strategy yielded in an overall sensitivity of 87% and a specificity of 97% (Fig. 2). For the majority vote classifier, all three biomarker values were equally weighted in the diagnostic decision process. Frequencies below the decisive threshold at 1643 cm^{-1} voted for AD. As soon as two biomarkers were below 1643 cm^{-1}, the final diagnostic decision of the classifier was AD.

In summary, step 1 of our two-step AD recruitment strategy identified individuals with a largely increased likelihood for AD based on blood plasma analyses. The second diagnostic step, based on CSF analyses, confirmed AD and excluded FP suggested by step 1. Thus, an overall diagnostic accuracy of 93% and a likelihood ratio (LR+) of 29 were observed for AD/non-AD differentiation relative to the CSF biomarker cross-validated clinical diagnosis.

4. Discussion

Already in 2016, we have discovered that Aβ can be used as a structure-based biomarker in a blood test [20]. In the following, the diagnostic performance of our structure-based biomarker was validated for mild to severe AD, prodromal AD, and even for preclinical AD 8 years before clinical symptoms occurred [20,22] in three independent clinical studies. Furthermore, the structure-based biomarker correlates with the Aβ42/40 ratio in CSF and with PET scanning [20,22]. However, the sensitivity and specificity of our blood test had to be increased for clinical application. In general, immuno-infrared analyses based on CSF showed a better diagnostic performance than blood-based analyses (see also Supplementary Fig. 5). This difference might be explained by different secondary structure stabilizing effects, Aβ concentrations, and the origin of Aβ generation in blood

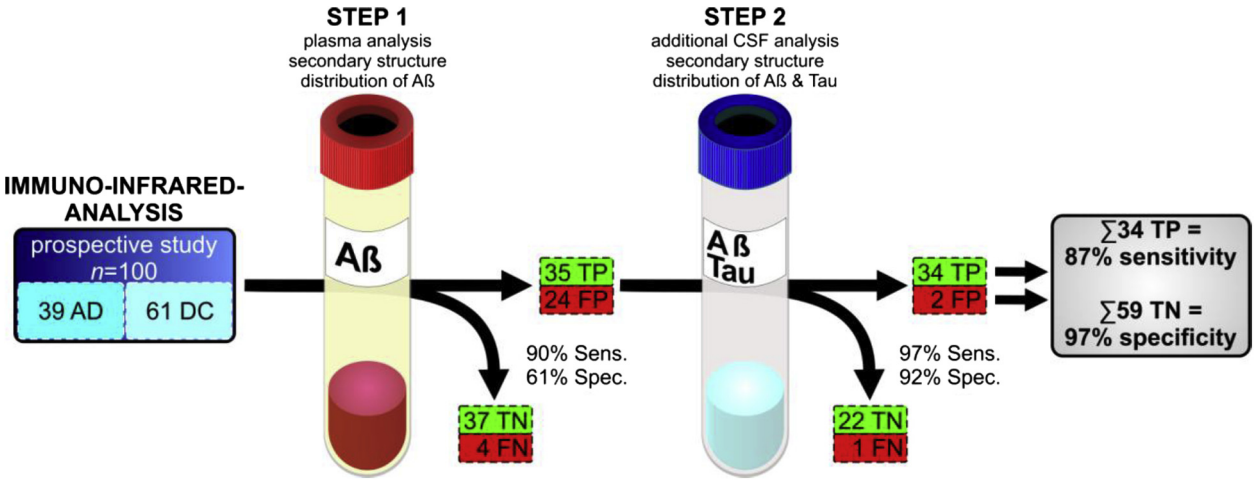

Fig. 2. Procedure of the two-step AD recruitment strategy. In step 1, the structure-based biomarker was analyzed in blood plasma of 61 DC and 39 AD patients by the immuno-infrared sensor. As a result, 37 true-negatives (TN), 4 false-negatives (FN), 35 true-positives (TP), and 24 false-positives (FP) were identified in step 1 (sensitivity 90%, specificity 61%). In step 2, CSF of positive-tested individuals was analyzed regarding the Aβ and tau secondary structure distribution. Therewith, AD diagnosis could be confirmed in 34 of 35 cases. On the other hand, FP could be excluded in 22 of 24 cases, thus only two FP remained (sensitivity 97%, specificity 92%). This yielded in an overall sensitivity of 87% and a specificity of 97%.

plasma. However, here we show that the immuno-infrared sensor–based two-step AD recruitment strategy can be used to identify AD with an overall sensitivity of 87% and specificity of 97%. Therefore, in addition to Aβ, tau also was used as a structure-based biomarker. This shows nicely that the specificity of the test is increased by use of other structure-based biomarkers. Hence, we will use the structure-based tau biomarker also in blood, as soon as we establish an antibody for tau detection in blood in our assay. The blood test can be applied to identify subjects with high probability for AD in a blood-based first step. The second step application of the immuno-infrared sensor substantially increases the diagnostic specificity, thus validating the final neurochemical diagnosis of AD. In the present study, most cases presented assured AD and the blood plasma–based immuno-infrared sensor offered in the first diagnostic step a sensitivity of 90%. Hence, the assay is suitable to identify patients with dementia due to AD. Subjects that were preselected in this first step entered a second step, where CSF was analyzed by the immuno-infrared sensor. Therewith, an overall specificity of 97% was obtained with only 2 FP of 61 DCs. Regarding the patient cohort, our study is limited by a challenge bias (STARDdem criteria) because only patients with cognitive decline have been investigated, and only patients with probable AD were included (possible AD excluded). At this disease stage, neuropsychiatrists may directly recommend a lumbar puncture to substantiate the AD diagnosis. But our previous studies clearly demonstrated that our immuno-infrared assay is already able to detect preclinical disease stages. Thus, we have evidence that the two-step diagnostic process can also be applied to recruit individuals in asymptomatic disease stages. The two-step procedure presents a promising recruitment strategy for the preselection of individuals for clinical prevention trials focusing on the Aβ and/or tau as a therapeutic target. We could demonstrate that our structure-based biomarker (Aβ) significantly correlates with Amyloid-PET scanning on prodromal AD cases and with neurochemical CSF biomarkers in previous studies [20,22]. In clinical practice, the two-step diagnostic process funnels individuals that may undergo comprehensive and expensive examinations such as lumbar puncture or brain imaging. However, for large prevention studies, the initial sensitive blood test will also be a reliable tool to preselect individuals with high risk for AD progression with a positive predictive value of 8 for study participation. This will also reduce the screening failure, that is, the number of individuals and costs that may undergo unnecessary comprehensive and expensive examinations such as lumbar puncture or brain imaging as recommended by FDA guidelines for clinical prevention studies.

Nevertheless, individuals who were preselected by our first blood plasma test may also be considered for conventional CSF-based neurochemical dementia diagnostics (measurement of Aβ40, Aβ42, ttau, and ptau levels) or for amyloid- or glucose-based PET to image Aβ burden or glucose dysmetabolism in the brain. Furthermore, the blood-based immuno-infrared sensor can also be combined with other promising novel blood tests for a two-step AD recruitment strategy [16–18]. For instance, Nakamura et al. [18] and Ovod et al. [17] previously reported mass-spectrometric approaches for the quantification of Aβ42/40 and Aβ669-711 levels in blood plasma. In clinical studies focusing on Aβ-PET–positive severe AD cases, both approaches revealed an accuracy of 85-90% with the Aβ-PET status. Most recently, Verberk et al. [16] focused on the identification of cognitively normal individuals with subjective cognitive decline, which converted to MCI or AD over years, by measuring the A42/40 ratio in blood plasma

using the Single Molecule Array technology. This approach resulted in the Amsterdam study in a diagnostic accuracy of 76% [16]. All technologies may be applied in combination to receive a powerful solely blood-based AD recruitment platform.

Acknowledgments

Prof. Jens Wiltfang is supported by an Ilídio Pinho professorship and iBiMED (UID/BIM/04501/2013), and FCT project PTDC/DTP_PIC/5587/2014 at the University of Aveiro, Portugal.

Supplementary Data

Supplementary data related to this article can be found at https://doi.org/10.1016/j.dadm.2019.01.008.

RESEARCH IN CONTEXT

1. Systematic review: There is an urgent need for a minimal-invasive blood test to identify patients with Alzheimer's disease (AD) for clinical studies/trials focusing on amyloid-β (Aβ). Such test would also reduce the number of individuals for invasive or expensive examinations. To date, guidelines recommend only CSF and PET analyses because of the lack of reliable blood tests.
2. Interpretation: The Aβ secondary structure distribution in plasma provides a sensitive biomarker for the preselection of individuals with increased probability for AD. Subsequent analyses of the Aβ and tau secondary structure distribution in CSF were efficient to confirm AD diagnoses and exclude false-positives with high diagnostic precision.
3. Future directions: Our two-step diagnostic process provides an alternative in AD diagnosis. Especially, the plasma analysis presents a minimal-invasive test for routine use to select individuals with increased probability for AD. Subsequent comprehensive examinations, e.g., our CSF-based procedure, standard ELISAs, and PET, can finally be arranged to confirm the diagnosis.

References

[1] Bateman RJ, Xiong C, Benzinger TLS, Fagan AM, Goate A, Fox NC, et al. Clinical and Biomarker Changes in Dominantly Inherited Alzheimer's Disease. N Engl J Med 2012;367:795–804.
[2] Rowe CC, Bourgeat P, Ellis KA, Brown B, Lim YY, Mulligan R, et al. Predicting Alzheimer disease with β-amyloid imaging: Results from the Australian imaging, biomarkers, and lifestyle study of ageing. Ann Neurol 2013;74:905–13.
[3] Wang Y, Mandelkow E. Tau in physiology and pathology. Nat Rev Neurosci 2016;17:5–21.
[4] Blennow K, de Leon MJ, Zetterberg H. Alzheimer's disease. Lancet 2006;368:387–403.
[5] Paraskevaidi M, Martin-Hirsch PL, Martin FL. Progress and Challenges in the Diagnosis of Dementia: A Critical Review. ACS Chem Neurosci 2018;9:446–61.
[6] Simonsen AH, Herukka SK, Andreasen N, Baldeiras I, Bjerke M, Blennow K, et al. Recommendations for CSF AD biomarkers in the diagnostic evaluation of dementia. Alzheimer's Dement 2017;13:274–84.
[7] Hendrix JA, Finger B, Weiner MW, Frisoni GB, Iwatsubo T, Rowe CC, et al. The Worldwide Alzheimer's Disease Neuroimaging Initiative: An update. Alzheimer's Dement 2015;11:850–9.
[8] McKhann GM, Knopman DS, Chertkow H, Hyman BT, Jack CR, Kawas CH, et al. The diagnosis of dementia due to Alzheimer's disease: Recommendations from the National Institute on Aging-Alzheimer's Association workgroups on diagnostic guidelines for Alzheimer's disease. Alzheimer's Dement 2011;7:263–9.
[9] Dubois B, Feldman HH, Jacova C, Hampel H, Molinuevo JL, Blennow K, et al. Advancing research diagnostic criteria for Alzheimer's disease: The IWG-2 criteria. Lancet Neurol 2014;13:614–29.
[10] Jack CR, Therneau TM, Wiste HJ, Weigand SD, Knopman DS, Lowe VJ, et al. Transition rates between amyloid and neurodegeneration biomarker states and to dementia: A population-based, longitudinal cohort study. Lancet Neurol 2016;15:56–64.
[11] Laske C, Sohrabi HR, Frost SM, López-De-Ipiña K, Garrard P, Buscema M, et al. Innovative diagnostic tools for early detection of Alzheimer's disease. Alzheimer's Dement 2015;11:561–78.
[12] Zhao X, Lejnine S, Spond J, Zhang C, Ramaraj TC, Holder DJ, et al. A candidate plasma protein classifier to identify Alzheimer's disease. J Alzheimer's Dis 2015;43:549–63.
[13] Mapstone M, Cheema AK, Fiandaca MS, Zhong X, Mhyre TR, Macarthur LH, et al. Plasma phospholipids identify antecedent memory impairment in older adults. Nat Med 2014;20:415–8.
[14] Snyder HM, Carrillo MC, Grodstein F, Henriksen K, Jeromin A, Lovestone S, et al. Developing novel blood-based biomarkers for Alzheimer's disease. Alzheimer's Dement 2014;10:109–14.
[15] Olsson B, Lautner R, Andreasson U, Öhrfelt A, Portelius E, Bjerke M, et al. CSF and blood biomarkers for the diagnosis of Alzheimer's disease: a systematic review and meta-analysis. Lancet Neurol 2016;15:673–84.
[16] Verberk IMW, Slot RE, Verfaillie SCJ, Heijst H, Prins ND, van Berckel BNM, et al. Plasma amyloid as pre-screener for the earliest Alzheimer's pathological changes. Ann Neurol 2018;138:1328–36.
[17] Ovod V, Ramsey KN, Mawuenyega KG, Bollinger JG, Hicks T, Schneider T, et al. Amyloid β concentrations and stable isotope labeling kinetics of human plasma specific to central nervous system amyloidosis. Alzheimer's Dement 2017;13:841–9.
[18] Nakamura A, Kaneko N, Villemagne VL, Kato T, Doecke J, Doré V, et al. High performance plasma amyloid-β biomarkers for Alzheimer's disease. Nature 2018;554:249–54.
[19] Fandos N, Pérez-Grijalba V, Pesini P, Olmos S, Bossa M, Villemagne VL, et al. Plasma amyloid β 42/40 ratios as biomarkers for amyloid β cerebral deposition in cognitively normal individuals. Alzheimer's Dement Diagnosis, Assess Dis Monit 2017;8:179–87.
[20] Nabers A, Ollesch J, Schartner J, Kötting C, Genius J, Hafermann H, et al. Amyloid-β-Secondary Structure Distribution in Cerebrospinal Fluid and Blood Measured by an Immuno-Infrared-Sensor: A Biomarker Candidate for Alzheimer's Disease. Anal Chem 2016;88:2755–62.
[21] Nabers A, Ollesch J, Schartner J, Kötting C, Genius J, Haußmann U, et al. An infrared sensor analysing label-free the secondary structure of the Abeta peptide in presence of complex fluids. J Biophotonics 2016;9:224–34.

[22] Nabers A, Perna L, Lange J, Mons U, Schartner J, Güldenhaupt J, et al. Amyloid blood biomarker detects Alzheimer's disease. EMBO Mol Med 2018;10:e8763.

[23] Noel-Storr AH, McCleery JM, Richard E, Ritchie CW, Flicker L, Cullum SJ, et al. Reporting standards for studies of diagnostic test accuracy in dementia: The STARDdem Initiative. Neurology 2014; 83:364–73.

[24] Lewczuk P, Zimmermann R, Wiltfang J, Kornhuber J. Neurochemical dementia diagnostics: A simple algorithm for interpretation of the CSF biomarkers. J Neural Transm 2009;116:1163–7.

Supplemental Materials for

2-Step Alzheimer's Disease Diagnosis: Plasma Aß as a Funnel for Subsequent CSF Aß and Tau Analyses

Andreas Nabers[1], Henning Hafermann[2], Jens Wiltfang[2,3,4], Klaus Gerwert[1]

[1]Department of Biophysics, Ruhr-University Bochum, 44801 Bochum, Germany
[2]Clinics for Psychiatry and Psychotherapie, LVR-Clinical Center Essen, 45147 Essen, Germany
[3]Department of Psychiatry and Psychotherapy, Georg-August-University Göttingen, University Medical Center, 37099 Göttingen, Germany
[4]German Center for Neurodegenrative Diseases (DZNE), 37099 Göttingen, Germany

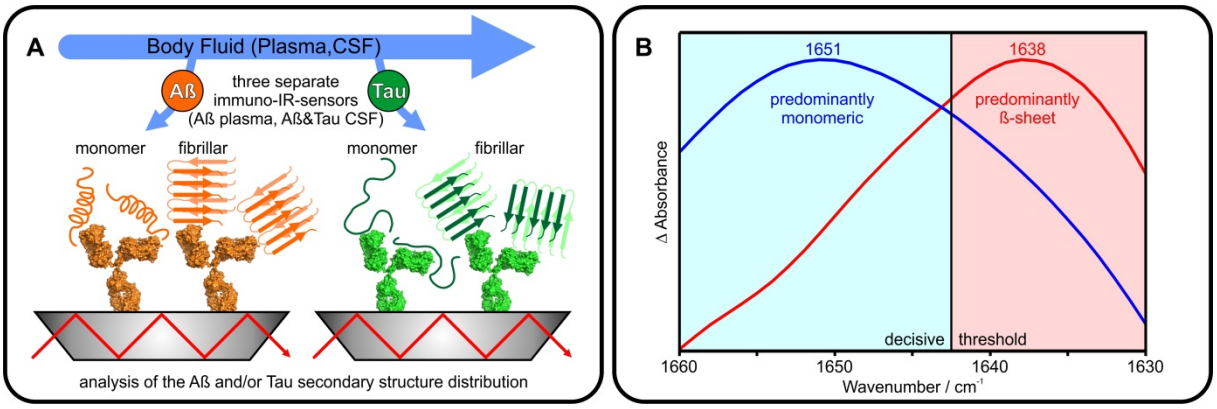

Supplemental Figure 1. (A) Three immuno-infrared-sensors were used to separately extract the Aß peptide fraction from blood plasma, the Aß peptide fraction from CSF, and the Tau protein fraction from CSF, respectively. For each biomarker the secondary structure sensitive amide I band was recorded, which is an integrated signal over all conformational isoforms of the biomarker (monomeric, oligomeric, and fibrillar isoforms of Aß in plasma, Aß in CSF, and Tau in CSF). (B) Depending on the content of ß-sheet enriched species (e.g. oligomers or fibrillar isoforms) in the total biomarker fraction the recorded amide I maximum frequency shifts to lower wavenumbers [1,2]. For each detected biomarker a decisive threshold for AD identification was determined. If the amide I frequency is below the threshold, the diagnosis will be AD, whereas a maximum above is indicative for non AD.

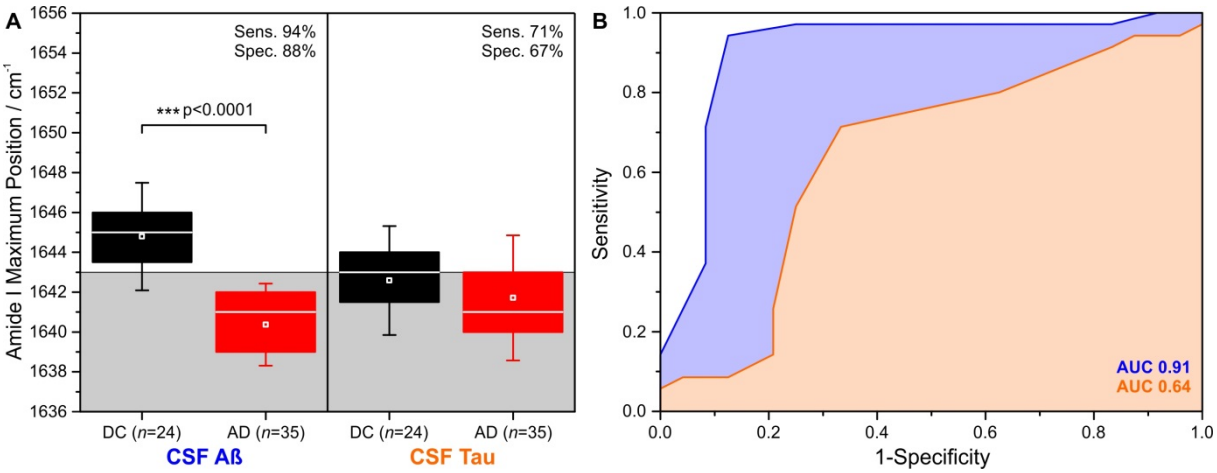

Supplemental Figure 2. (A) The amide I maximum frequencies of both Aß and Tau from CSF of 24 false-positive and 35 true-positive individuals, as determined by the first diagnostic procedure based on blood as shown in Figure 1, were displayed as box plots. Thereby, the maximum frequency represented the secondary structure distribution of the biomarker. For CSF Aß analyses, a decisive threshold <1643 cm^{-1} separated DC subjects and AD cases with a sensitivity 94% and a specificity of 88%. For CSF Tau analyses, the decisive threshold <1643 cm^{-1} separated DC subjects and AD cases with a sensitivity 71% and a specificity of 67%. (B) The corresponding ROC-curve analyses yielded area under curves (AUC) of 0.91 for Aß and 0.64 for Tau. Thus, the Tau secondary structure distribution in CSF is not suitable as a stand-alone diagnostic marker for Alzheimer's disease. Data information: In box plots, 25/50/75% quantiles are shown as horizontal lines, the average amide I band position as square, and ± standard deviation as whiskers. Significant group differences are indicated by *p*-values (two-sided nonparametric Kruskal–Wallis analysis of variance test) and by asterisks: *P < 0.05,**P < 0.01, ***P < 0.001.

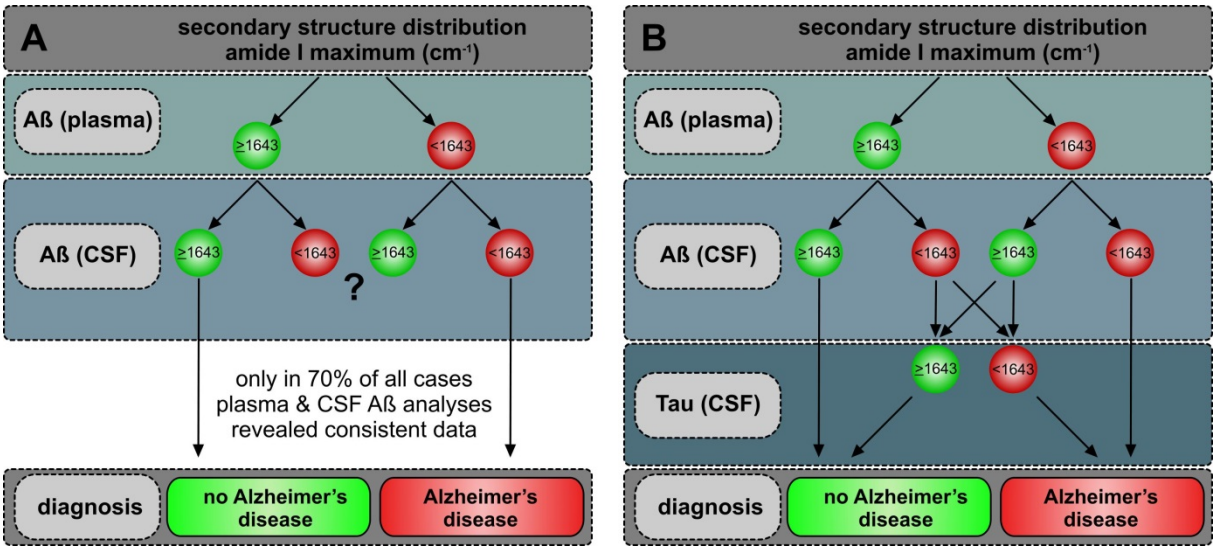

Supplemental Figure 3. Schematic representation of the principle of the majority vote classifier. For each individual, the amide I maximum of plasma Aß, CSF Aß, and CSF Tau was recorded. (A) In 70% of all investigated cases the recorded amide I maximum of Aß from plasma and CSF was consistently above or below the discriminating threshold <1643 cm^{-1}. For this percentage, AD vs. non AD differentiation could be directly made with high diagnostic accuracy. (B) For inconsistent data the Tau amide I maximum frequency was considered to built-up a simple majority vote classifier. All biomarker values were equally weighted. If the amide I maximum of two biomarkers was below the threshold, the diagnosis was AD If the amide I maximum of two biomarkers was above the threshold, AD was excluded (see also Supplemental Figure 4 and Figure 2).

Step 2 of AD diagnostics (blood&CSF)
(exclusion of FP & ensuring of TP)

DC #	Aß plasma AD<1643 cm^{-1}	Aß CSF DC ≥ 1643 cm^{-1}	Tau CSF	majority vote DC	majority vote AD
1	1638	1652	1643		
2	1639	1643	1645	●	
3	1639	1643	1641		●
4	1640	1642	1648		●
5	1642	1646	1643	●	
6	1642	1645	1643	●	
7	1643	1647	1637	●	
8	1643	1639	1643	●	
9	1643	1644	1644	●	
10	1644	1646	1642	●	
11	1644	1646	1644	●	
12	1644	1643	1638	●	
13	1645	1644	1643	●	
14	1645	1644	1639	●	
15	1645	1646	1643	●	
16	1645	1644	1644	●	
17	1645	1639	1644	●	
18	1646	1647	1643	●	
19	1646	1646	1646	●	
20	1646	1645	1642	●	
21	1646	1645	1644	●	
22	1646	1645	1639	●	
23	1646	1646	1638	●	
24	1646	1648	1646		

Majority vote decision:

2 biomarker values <1643 cm^{-1} = AD ●
2 biomarker values ≥1643 cm^{-1} = DC ●

AD #	Aß plasma AD<1643 cm^{-1}	Aß CSF DC ≥ 1643 cm^{-1}	Tau CSF	majority vote DC	majority vote AD
1	1637	1641	1639		●
2	1638	1639	1639		●
3	1638	1641	1653		●
4	1638	1639	1640		●
5	1638	1639	1640		●
6	1638	1642	1635		●
7	1638	1641	1644		●
8	1639	1638	1637		●
9	1639	1642	1642		●
10	1640	1642	1641		●
11	1640	1642	1644		●
12	1640	1639	1641		●
13	1640	1641	1642		●
14	1641	1641	1642		●
15	1641	1642	1648		●
16	1641	1640	1642		●
17	1641	1637	1643		●
18	1641	1639	1641		●
19	1641	1639	1641		●
20	1641	1643	1642		●
21	1641	1636	1641		●
22	1641	1647	1640		●
23	1641	1641	1640		●
24	1641	1637	1645		●
25	1642	1639	1636		●
26	1642	1639	1641		●
27	1642	1642	1641		●
28	1642	1641	1643		●
29	1642	1642	1644		●
30	1642	1641	1643		●
31	1643	1638	1644	●	
32	1643	1642	1641		●
33	1644	1640	1642		●
34	1645	1641	1641		●
35	1646	1640	1642		●

Supplemental Figure 4. After the first diagnostic step based on blood plasma as shown in Figure 1, 24 false-positives and 35 true-positives were considered for subsequent CSF analyses in a second diagnostic step. Thereby, additionally the secondary structure sensitive amide I band of Aß and Tau in CSF was recorded. AD was indicated if the amide I maximum frequency was below the decisive threshold at <1643 cm^{-1}. If the amide I maximum of two biomarkers was below the threshold, the diagnosis of the majority vote classifier was AD. If the amide I maximum of two biomarkers was above the threshold, AD was excluded (see also Supplemental Figure 3 and Figure 2). Therewith, only two out of 24 DC remain as false-positives (red dots in the DC group, left), whereas AD diagnosis of 34 out of 35 cases could be confirmed (only one false-negative in the AD group, right).

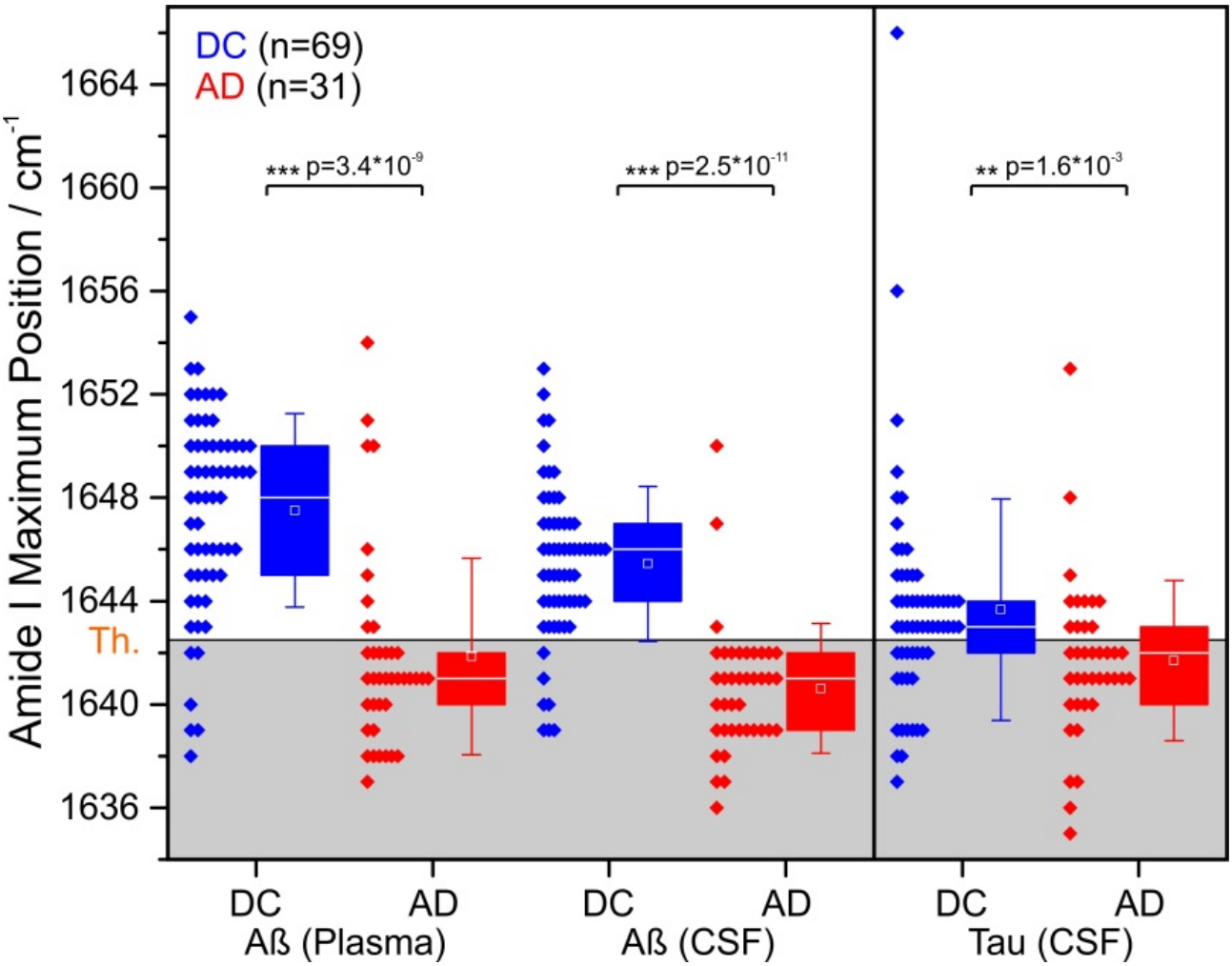

Supplemental Figure 5. The amide I maximum frequencies of Aß in plasma, Aß in CSF, and Tau in CSF of 69 DC and 31 AD cases (total population of the prospective cohort) were displayed as box plots, data points were illustrated as diamonds. Thereby, the maximum frequency represented the secondary structure distribution of the biomarker. In former studies 1643 cm^{-1} was experimentally determined as decisive threshold (Th.) for highest test accuracy. For all three biomarkers the amide I maximum frequency differed significantly within the total study population. Additionally to Figure S2, we measured the secondary structure distribution of CSF-Tau with our immuno-infrared-sensor of all participants including the individuals of step 1 that were not selected for step 2. Within the whole population (100 individuals) CSF-Tau significantly differed between DC subjects and AD cases with $p=1.6*10^{-3}$. Further significant group differences between DC and AD were $3.4*10^{-9}$ for Plasma Aß and $2.5*10^{-11}$ for CSF Aß. Data information: In box plots, 25/50/75% quantiles are shown as horizontal lines, the average amide I band position as square, and ± standard deviation as whiskers. Significant group differences are indicated by p-values (two-sided nonparametric Kruskal–Wallis analysis of variance test) and by asterisks: *P < 0.05,**P < 0.01, ***P < 0.001.

Supplemental Table 1. Phenotyping data of the patient collective, including the dementia biomarkers and the amide I maximum position of Aß and Tau of DC (A) and AD patients (B).

A Patient #	Age	Sex (m/f)	MMSE	Aß1-42 [pg/ml]	Aß1-42/1-40 ratio	MSD ratio Aß42/40	phospho-Tau [pg/ml]	total-Tau [pg/ml]	Amide I plasma Aß [cm^{-1}]	Amide I CSF Aß [cm^{-1}]	Amide I CSF Tau [cm^{-1}]
1	67	m	29	1063	n.a.	0.114	46	211	1653	1646	1645
2	87	m	12	681	n.a.	0.05	69.1	339	1644	1646	1642
3	80	f	30	637	n.a.	0.113	34.5	<75	1649	1649	1644
4	52	m	30	827	n.a.	0.128	26.6	<75	1650	1646	1656
5	62	m	28	620	n.a.	0.119	<15.6	100	1652	1647	1666
6	80	m	n.a.	712	n.a.	0.076	57	292	1655	1651	1645
7	56	f	6	675	n.a.	0.08	47.7	368	1650	1650	1643
8	80	m	20	637	n.a.	0.083	53.6	214	1650	1644	1642
9	87	f	19	714	n.a.	0.075	38.4	281	1650	1651	1645
10	67	f	21	1095	0.0992	0.127	36.1	165	1649	1647	1642
11	62	m	n.a.	875	0.0554	0.087	38	206	1642	1646	1643
12	56	f	n.a.	1997	0.1164	0.112	48.1	218	1646	1647	1643
13	42	f	n.a.	1410	n.a.	0.118	63.8	247	1644	1646	1644
14	70	f	28	980	n.a.	0.109	22.5	112	1646	1646	1646
15	57	m	25	1064	0.1319	0.11	23.4	109	1650	1644	1642
16	68	m	26	1795	0.0991	0.111	44.2	275	1651	1640	1641
17	65	m	n.a.	485	0.0486	0.048	52.4	327	1650	1641	1643
18	68	m	23	644	0.0535	0.044	94.8	483	1645	1644	1643
19	57	f	n.a.	1664	0.0993	0.119	42.3	174	1639	1643	1645
20	62	f	24	1423	0.0807	0.112	49.3	190	1648	1644	1642
21	89	f	16	477	n.a.	0.057	41.8	233	1645	1644	1639
22	82	f	20	1109	0.1010	0.107	38.3	220	1643	1647	1637
23	74	m	24	839	n.a.	0.074	58	311	1644	1643	1638
24	74	f	25	1192	0.0716	0.072	65.4	308	1647	1643	1639
25	55	m	27	1798	0.0866	0.12	92.3	356	1646	1645	1642
26	60	m	30	1537	0.0991	0.12	80.2	303	1650	1646	1641
27	67	m	27	1147	0.0501	0.08	92.8	363	1649	1649	1643
28	69	m	29	1418	0.0636	0.127	54.4	289	1638	1652	1643
29	83	f	n.a.	820	0.0655	0.072	43.7	286	1652	1646	1649
30	54	f	29	1877	0.0687	0.13	52.4	276	1646	1645	1644
31	60	m	30	605	0.1348	0.123	<15.6	140	1649	1647	1644
32	71	m	10	1048	0.0905	0.102	45.3	243	1651	1644	1645
33	53	f	28	n. a.	n.a.	0.11	n.a.	n.a.	1649	1653	1641
34	82	m	28	1324	0.1126	0.12	39.7	242	1646	1645	1639
35	92	f	20	731	0.0685	0.068	49.6	273	1652	1645	1648
36	77	f	20	731	0.0540	0.065	53.3	275	1649	1648	1643
37	70	f	n.a.	1773	0.0587	0.126	93.1	481	1649	1645	1644
38	61	m	29	1431	0.0887	0.119	42.1	328	1650	1647	1644
39	85	f	n.a.	1604	0.0707	0.123	71.3	316	1648	1649	1644
40	50	f	22	1563	0.0837	0.121	37.5	209	1648	1645	1643
41	63	f	30	1457	0.0723	0.098	53.6	296	1652	1643	1644
42	75	m	24	930	0.0415	0.06	62.9	355	1652	1646	1644
43	79	f	13	978	0.0859	0.1	52.1	364	1648	1647	1639
44	66	f	13	1114	0.1017	0.114	25.2	267	1651	1648	1639
45	78	f	29	1537	0.0601	0.12	53.1	299	1651	1640	1643
46	78	m	27	1498	n.a.	0.085	96.2	412	1643	1639	1643
47	44	f	27	1521	0.0907	0.121	25.1	126	1646	1646	1638
48	88	f	21	1119	0.0499	0.099	57.2	378	1645	1646	1643
49	81	f	13	862	0.0631	0.084	60.3	325	1649	1646	1646
50	84	f	n.a.	1158	0.1034	0.125	27.7	150	1648	1646	1651
51	83	m	25	1982	0.0988	0.115	65	374	1647	1648	1644
52	71	m	27	1933	0.1170	0.113	53.6	292	1653	1644	1639
53	70	f	28	1169	0.0629	0.064	54.2	272	1642	1645	1643
54	61	m	n.a.	890	0.0778	0.104	59.5	291	1649	1643	1642
55	74	m	28	1655	0.0943	0.118	68.4	305	1639	1643	1641
56	65	m	26	1127	0.1178	0.107	40.8	239	1645	1644	1644
57	66	m	29	1722	0.0987	0.097	59.2	311	1646	1648	1646
58	44	m	30	1351	0.1144	0.107	41.8	169	1640	1642	1648
59	69	f	27	1201	0.0772	0.108	31.1	134	1643	1644	1644
60	75	m	n.a.	n.a.	n.a.	0.113	n.a.	n.a.	1650	1639	1647
61	58	f	n.a.	742	0.0603	0.105	33.3	190	1645	1639	1644
mean	68		24	1169	0.0831	0.100	50.7	262	1648	1645	1644
std ±	12		6	421	0.0238	0.023	19.2	92	4	3	4
min value	42		6	477	0.0415	0.044	15.6	75	1638	1639	1637
max value	92		30	1997	0.1348	0.130	96.2	483	1655	1653	1666

Supplemental Table 1. Phenotyping data of the patient collective, including the dementia biomarkers and the amide I maximum position of Aß and Tau of DC (A) and AD patients (B).

B Patient #	Age	Sex (m/f)	MMSE	Aß1-42 [pg/ml]	Aß1-42/1-40 ratio	MSD ratio Aß42/40	phospho Tau [pg/ml]	total Tau [pg/ml]	Amide I plasma Aß [cm^{-1}]	Amide I CSF Aß [cm^{-1}]	Amide I CSF Tau [cm^{-1}]
62	78	m	22	837	n.a.	0.060	69.1	436	1654	1650	1642
63	61	m	25	455	0.0213	0.040	169	>1200	1650	1640	1644
64	79	f	22	525	n.a.	0.043	123	600	1637	1641	1639
65	81	f	19	640	n.a.	0.063	79.1	414	1641	1641	1642
66	69	f	21	587	n.a.	0.031	275	>1200	1640	1642	1641
67	57	m	16	541	0.0548	0.070	62.8	256	1641	1642	1648
68	55	f	22	558	0.0275	0.060	101	790	1643	1638	1644
69	79	m	18	561	0.0221	0.059	74.5	450	1650	1642	1637
70	58	m	17	664	n.a.	0.042	162	980	1640	1642	1644
71	71	f	26	597	0.0391	0.053	119	950	1641	1640	1642
72	73	f	26	675	0.0331	0.052	72.2	355	1642	1639	1636
73	73	f	20	596	0.0440	0.046	87.7	349	1641	1637	1643
74	67	f	26	530	0.0303	0.034	129	667	1644	1640	1642
75	56	f	n.a.	593	0.0478	0.056	106	914	1638	1639	1639
76	79	f	16	963	0.0455	0.063	147	1050	1641	1639	1641
77	70	m	27	577	0.0257	0.039	69.5	469	1641	1639	1641
78	78	f	n.a.	582	0.0625	0.062	64.5	417	1641	1643	1642
79	86	f	19	643	0.0510	0.059	90.6	420	1638	1641	1653
80	58	f	25	856	0.0355	0.045	194	>1200	1639	1638	1637
81	85	m	n.a.	819	0.0235	0.045	173	>1200	1641	1636	1641
82	60	f	29	638	0.0272	0.037	109	735	1641	1647	1640
83	79	f	17	522	0.0310	0.040	91.7	944	1642	1639	1641
84	78	m	12	888	0.0393	0.055	113.4	877	1642	1642	1641
85	75	f	23	612	n.a.	0.051	115.8	1114	1638	1639	1640
86	72	f	12	n.a.	n.a.	0.051	n.a.	n.a.	1640	1639	1641
87	62	f	27	782	0.0412	0.052	82.7	554	1651	1639	1643
88	68	f	n.a.	464	0.0259	0.037	131	>1200	1638	1639	1640
89	72	m	22	787	0.0395	0.061	112	>1200	1641	1641	1640
90	78	f	24	515	n.a.	0.043	110	627	1645	1641	1641
91	87	f	22	610	0.0450	0.049	172	>1200	1643	1642	1641
92	69	f	10	832	0.0456	0.058	76.9	482	1646	1640	1642
93	65	m	16	1052	0.0529	0.067	84.9	424	1639	1642	1642
94	79	f	24	801	0.0665	0.059	66.6	423	1642	1641	1643
95	70	f	26	675	0.0650	0.044	109	772	1640	1641	1642
96	92	f	24	551	0.0315	0.034	136	882	1638	1642	1635
97	68	m	15	728	0.0369	0.050	91.1	465	1641	1637	1645
98	76	f	27	116	n.a.	0.043	15.6	<75	1638	1641	1644
99	51	f	25	474	0.0354	0.054	88	680	1642	1642	1644
100	68	f	24	469	0.0200	0.039	125	>1200	1642	1641	1643
mean	71		21	640	0.0392	0.050	110.5	741	1642	1641	1642
std ±	10		5	170	0.0134	0.010	46.0	333	4	3	3
min value	51		10	116	0.0200	0.031	15.6	75	1637	1636	1635
max value	92		29	1052	0.0665	0.07	275	1200	1654	1650	1653

Cutoff-values for AD diagnosis were <600 pg/ml for Aß42, <0.05 for Aß42/40 ratio (ELISA), <0.0635 for Aß42/40 ratio (MSD), >60 pg/ml for phospho-Tau, >300 pg/ml for total-Tau. MMSE were 27-30=cognitive unimpaired, 26=mild dementia, 10-19=moderate dementia, and <10=severe dementia.

References

[1] Nabers A, Ollesch J, Schartner J, Kötting C, Genius J, Hafermann H, et al. Amyloid-β-Secondary Structure Distribution in Cerebrospinal Fluid and Blood Measured by an Immuno-Infrared-Sensor: A Biomarker Candidate for Alzheimer's Disease. Anal Chem 2016;88. doi:10.1021/acs.analchem.5b04286.

[2] Nabers A, Perna L, Lange J, Mons U, Schartner J, Güldenhaupt J, et al. Amyloid blood biomarker detects Alzheimer's disease. EMBO Mol Med 2018;10:e8763. doi:10.15252/emmm.201708763.